FOREX Publication
Open Access | Rapid and quality publishing

International Journal of
Electrical and Electronics Research (IJEER)
Research Article | Volume 12, Issue 2 | Pages 487-492 | e-ISSN: 2347-470X

Analysis of Disc Motor with Asymmetrical Conducting Rotor

Ahmed Samir Kheder[1*], M. A. Elwany[2] and A. B. Kotb[3]

[1]*Department of Electrical Engineering, Faculty of Engineering and Technology, Future University in Egypt, Cairo, Egypt; EG95AhmedSamir@gmail.com*
[2]*Department of Electrical Engineering, Faculty of Engineering, Al-Azhar University, Cairo, Egypt; MahmoudHosain1712.el@azhar.edu.eg*
[3]*Department of Electrical Engineering, Faculty of Engineering, Al-Azhar University, Cairo, Egypt; moabdelsamie45@yahoo.com*

***Correspondence:** Ahmed Samir Kheder; EG95AhmedSamir@gmail.com

ABSTRACT- The homogenous disc rotor construction allows higher rotational speeds and relatively higher power densities. This paper deals with a two-phase induction motor with homogenous disc rotor construction. The field analysis of an axial flux disk motor with a conducting disc rotor is carried out, using a new application of the Maxwell's field equations. A Suggested model is introduced to establish the geometry of motor construction and to enable the derivation of the field system differential equations. A new strategy is applied for the boundary conditions to complete the field solution. This is carried out by determining the complex integration constants. The current density is completely derived with it is components (the radial, the tangential current density and the axial air gap flux density).

The performance of the flux density, rotor current components and the torque-slip characteristics are determined with and without disk rotor ends. The effects of the disk rotor design data and the rotor asymmetry on the motor performance are investigated.

Keywords: Induction motor; disc motor; axial flux; field equation; Electric Loading.

ARTICLE INFORMATION

Author(s): Ahmed Samir Kheder, M. A. Elwany and A. B. Kotb;
Received: 16/03/2024; **Accepted**: 10/05/2024; **Published**: 25/05/2024;
e-ISSN: 2347-470X;
Paper Id: IJEER 0812-03;
Citation: 10.37391/IJEER.120221
Webpage-link:
https://ijeer.forexjournal.co.in/archive/volume-12/ijeer-120221.html

Publisher's Note: FOREX Publication stays neutral with regard to Jurisdictional claims in Published maps and institutional affiliations.

1. INTRODUCTION

The induction disk motor, has a main stator disc, carrying the normal polyphase windings, embedded in radially directed slots of a laminated iron core. The disc motor has a flat circular conducting disc as rotor, which has asymmetrical ends compared to stator ends (the diameter of the rotor can be smaller, bigger or equal to the diameter of stator) as shown in *fig. 1*. If the disc motor with a conducting disc rotor is compared with the conventional cylindrical induction motors, their constructions, higher rotational speed, and the power density are the main differences, the homogenous disc construction allows higher rotational speeds corresponding to relatively higher power densities. Moreover, the disc motor has a relatively small mechanical time constant corresponding to its small moment of inertia [1]. These possibilities are the great advantages of using the disc motor in electrical controlled drive applications.

To tackle the multi-category issue in steel surface defects, this paper leveraged the EfficientNet network to replace the Yolov5 backbone. The feature maps of three scales of steel surface defects were extracted through the EfficientNet network, and then fused by the feature pyramid structure in the Yolov5 network to improve the overlapping target detection ability. We conducted comparative experiments involving EfficientNetB0-B7 and Yolov5 to assess fusion effects.

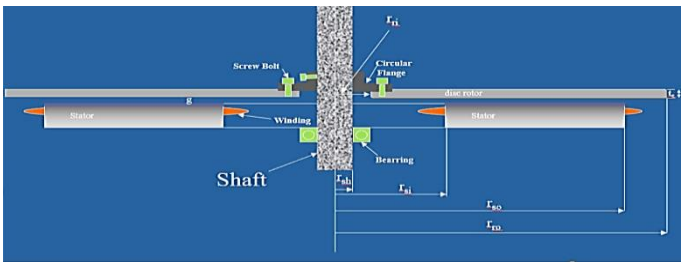

(a) 2D dimensions

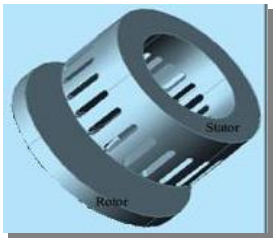

(b) 3D dimensions

Figure 1. Disk Motor, with Asymmetrical Disc Rotor (if the rotor diameter is bigger than the stator diameter)

FOREX Publication
Open Access | Rapid and quality publishing
International Journal of Electrical and Electronics Research (IJEER)
Research Article | Volume 12, Issue 2 | Pages 487-492 | e-ISSN: 2347-470X

Some authors have studied the disc rotor induction motor theoretically and experimentally. Analytical solution of the field problem is given in [2] assuming an idealized one-dimensional current density in the rotor disc.

A very simplified analysis using a linear model is given, some test results and a speed-controlled of disc motor are carried out [3]. Novotny introduced a two-phase accelerometer in a way that depends on knowing the data of the torque-speed in steady state and the rotor time constant [4]. A two-dimensional current distribution is considered in [1].

In this paper, the field analysis is carried out using a new application for the Maxwell's field equations, using simplified model. The current density in the disc rotor has been analyzed into tangential and radial components, while we assumed a constant magnetic flux density along the length of the air gap [5]. A new geometrical technique is applied for the boundary conditions to determine the complex integration constants.

The magnetic field density distribution and the rotor current density distribution are determined. The motor performance characteristics are given, and the results are discussed for different rotor design.

LIST OF SYMBOLS

A_s = stator electric loading	r_m =the stator main radius
r = radial coordinate	p = number of pole pairs
z, φ,r = coordinates	ω = angular frequency.
a_φ, a_r, a_z= unit vector	f = frequency,
B = flux density	ν = linear speed
J = rotor current density	σ = disc-rotor conductivity
t = time	s = slip
r_s = radius of the stator	E = electric field intensity
r_r = radius of the rotor	t_c = thickness of the rotor,
D1, D2 = the complex quantities of the integration constants.	K^2, c = complex quantity
r_{si}, r_{so} = inner and outer stator radius,	r_{ri}, r_{ro} = inner and outer rotor radius,
r_{sh} = the shaft radius	F_v = force density
A_{sm} =the amplitude of the fundamental stator electric loading wave at r_m	g_s = the air gap between the stator and rotor.
d_i = the difference between inner stator and inner rotor radius	T = torque
d_o= the difference between outer stator and outer rotor radius,	

2. THE STATOR ELECTRIC LOADING

As known, it is evident that knowing the electric loading of the stator is necessary for the magnetic field analysis to simplify the mathematical analysis, the height of the stator coils is assumed to be negligibly small and the distributed stator winding is replaced by a current sheet carrying the stator electric loading. Usually, the excitation system which produces the rotating magnetic field is consisting of poly-phase windings. Each phase windings for disc motor are embedded in radial direction in slots of a laminated iron core of one stator side. Thus, both stator electric loadings and the corresponding flux density waves are functions of time t, stator radius r and the peripheral angle **φ**. Generally, the electric loading A_s wave of the first stator phase at any r, can be expressed in the form

$$A_{s1}(r, \varphi, t) = \mathrm{Re}\{A_{s1}(r)\, e^{j(wt-\varphi)}\}, \quad (1)$$

Figure 2, is the redial distribution of stator electric loading from r_{si} to r_{so},
Which has a main value with complex amplitude

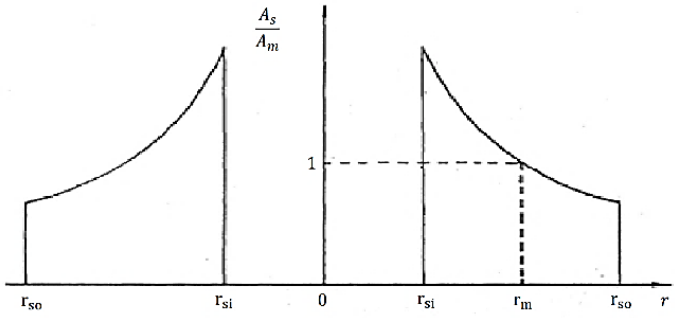

Figure 2. Redial Distribution of Stator Electric Loading

$$A_{sm} = A_{s1}.(\frac{r_m}{r}) \quad (2)$$

Where, A_{sm} is the amplitude of the fundamental stator electric loading wave at the stator main radius r_m

$$\text{With } r_m = (r_{si} + r_{so})/2 \quad (3)$$

we use the average A_{sm} as A_s by ignore it is variation with radius to simplify the analysis.

3. THE FIELD ANALYSIS

The following assumptions are taken into account in the analysis:

- A current sheet with extremely small thickness is represented the stator windings. This sheet carries the electric loading of the stator which placed on the stator smooth iron surface.
- The iron parts are assumed to be highly magnetic and non-conductive.
- The geometrical air gap between the two stator sides is so small, that the variation of the magnetic field in the axial direction can be ignored.
- Current density through the disc rotor has axial and tangential components.
- Only the axial component of the flux density, is considered (because this component is more effective).

FOREX Publication
Open Access | Rapid and quality publishing
International Journal of Electrical and Electronics Research (IJEER)
Research Article | Volume 12, Issue 2 | Pages 487-492 | e-ISSN: 2347-470X

3.1. Model for the Field Analysis

A simplified model will be used for the asymmetrical disc rotor induction motor to show us the field analysis. An approximate estimation of the field outside the inner and outer stator active region of lengths di and do, is introduced in the analysis. The relatively complex structure of the cylindrical disk rotor machine will be simplified for the purpose of our analysis and represented by the developed model shown in *figure. 3*.

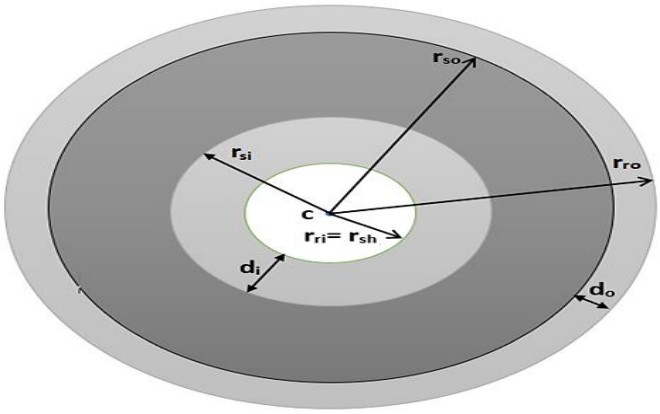

Figure 3. An Idealized Model of Disk Motor with Asymmetrical Rotor Ends) if the rotor diameter is bigger than the stator diameter)

3.2. The Field equations

Referring to the previous assumptions, the flux density of the air-gap has only its axial component

$$\vec{B} = B_z \vec{a_z} \tag{4}$$

Also, the disc-rotor current density has two components; radial and tangential J_r and J_φ respectively.

By applying the Maxwell's first equation in its integral form to the loop in *figure. 3*, of infinitesimal dimensions in polar coordinates gets

$$\frac{\partial B_z}{\partial \varphi} = \frac{\mu_o}{g_s}\,(r_s\,A_s + r_r\,t_c\,J_r) \tag{5}$$

Where r_s is the radius of the stator and r_r is the radius of the rotor.

The electric loading of the stator A_s is function of angle φ and time t , it can be represented by the following complex equation

$$A_s(t,\varphi) = \mathrm{Re}\{A_s\, e^{j(wt-P\varphi)}\} \tag{6}$$

where P is the pole pairs number and φ is the mechanical angle in degrees. At steady state, the flux density can be represented by [7]

$$B_z(r,\varphi,t) = \mathrm{Re}\{B_z(r)\, e^{j(wt-P\varphi)}\} \tag{7}$$

The rotor has two current density components, radial component J_r and tangential component J_φ, as

$$J_r(r,\varphi,t) = \mathrm{Re}\{J_r(r)\, e^{j(wt-P\varphi)}\} \tag{8}$$

By substitutions, the air gap flux density is then,

$$B_z(r) = j\frac{\mu_o r_s}{Pg_s} A_s + j\frac{\mu_o t_c r_r}{Pg_s} J_r \tag{9}$$

The general formula of current density for a moving conductor with *v* velocity, in an isotropic medium, is given by

$$\vec{J} = \sigma_c(\vec{E} + \vec{v} \times \vec{B}) \tag{10}$$

Where $\vec{E}$ is the electric field intensity due to static induced emf and σ_c is the conductivity of disc rotor.

Applying the second Maxwell's equation to the closed loop in *fig. 3*, gives

$$\frac{\partial J_\varphi}{\partial r} + j\frac{P}{r_r} J_r = j\omega\sigma_c s B_z(r) \tag{11}$$

The relation between the two components of the rotor current density (φ and r) can be obtained from the continuity condition, div J = 0.

Then $$J_\varphi = -j\frac{r_r}{P}\frac{\partial J_r}{\partial r} \tag{12}$$

From the proceeding relations, the radial component of the disc rotor current density is given by the following 2nd order differential equation

$$\frac{\partial^2 J_r}{\partial r^2} - \left[\frac{p^2}{r_s^2} - j\frac{\omega\sigma s\mu_o t_c}{g_s}\right] J_r = -j\frac{\omega\sigma s\mu_o}{g_s} A_s \tag{13a}$$

This can be written as $$\frac{\partial^2 J_r}{\partial r^2} - k^2 J_r = -C \tag{13b}$$

With $k^2 = \frac{p^2}{r_s^2} - j\frac{\omega\sigma s\mu_o t_c}{g_s}$ and $C = j\frac{\omega\sigma s\mu_o}{g_s} A_s$ (13c, d)

The above differential equation describes the rotor current density within the active stator width [15].

The second order differential equation (13a) describes the radial component of the disc rotor current density. *Equations, (9,11 and 12)* describes the relations between B_z , J_φ and J_r.

3.3. The field equations Solution

The operation of disk-rotor induction motors, linear induction motors, and MHD induction machines is based on the same physical principles. Since extensive studies of the latter two machines have been done, it is reasonable to apply these well-known analytical techniques to the first machine. In fact, a simple solution for the disk motor was obtained by integrating the differential equation of a linear induction motor after it was rewritten in cylinder coordinates and adapted to the modified boundary conditions [14].

A convenient general solution for the radial component of the current density J_r of equation (13a) is

$$J_r(r) = D_1 e^{kr} + D_2 e^{-kr} + \frac{C}{K^2} A_s \tag{14}$$

FOREX Publication
Open Access | Rapid and quality publishing
International Journal of Electrical and Electronics Research (IJEER)
Research Article | Volume 12, Issue 2 | Pages 487-492 | e-ISSN: 2347-470X

with the complex quantities D1 and D2 are the integration constants.

The complex constants D1 and D2 can be evaluated by applying the boundary conditions of Jr at the edges of the rotor-ends (r_{ri}, r_{ro}). The condition of continuity of current is now applied at every side of the rotor-ends.

Figure 4 shows the transition of the rotor current density from the active length to the disc-rotor ends. The tangential current density J_φ in the disc-rotor end region may be assumed constant along the rotor end width d_o (the outer ring width).

The radial current density component Jr turns to be tangential through the rotor-rings

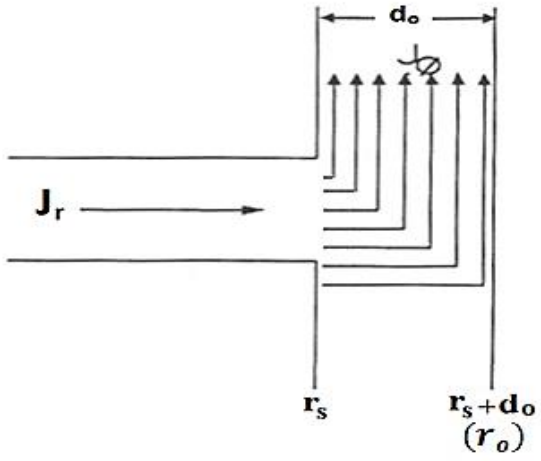

Figure 4. The Transition of Disc Rotor Current to the Rotor Ends

The continuity equation of the disc-rotor current at one rotor end region is applied to give,

$$J_\varphi(r_{si})\, t_c\, d_i = J_r(r_{si})\, t_c\, r_{si}\, \partial\varphi \quad (15)$$

Where d_i is the inner ring width, t_c is the disc rotor thickness.

then $$J_r(r_{si}) = \frac{d_i}{r_{si}} \frac{\partial J_\varphi(r_{si})}{\partial \varphi} \quad (16)$$

From the diversion theorem $$\frac{\partial J_\varphi}{r_{si}\partial\varphi}\Big|_{r_{si}} = \frac{\partial J_r}{\partial r}\Big|_{r_{si}} \quad (17a)$$

The condition of continuity of rotor current is now applied at the outer end side of the disc rotor active radius r_{so} to be

$$\frac{\partial J_\varphi}{r_{so}\,\partial\varphi}\Big|_{r_{so}} = \frac{\partial J_r}{\partial r}\Big|_{r_{so}} \quad (17b)$$

The integration constants are then,

$$D_1 = \frac{a_3}{a_1 + a_2} \quad (18a)$$

and $$D_2 = \frac{-\frac{c}{k^2}A_s - e^{kr_{so}}(1+d_o k)D_1}{e^{kr_{si}}(1+d_o k)} \quad (18b)$$

Where $$a_1 = \frac{e^{kr_{so}}(1+d_o k) - e^{kr_{si}}(1+d_i k)}{e^{kr_{so}}(1-d_i k) - e^{kr_{si}}(1-d_o k)} \quad (19a)$$

$$a_2 = \frac{e^{kr_{so}}(1+d_o k)}{e^{kr_{si}}(1-d_o k)} \quad (19b)$$

$$a_3 = \frac{c}{K^2} A_s \frac{e^{kr_{so}}}{(1-d_o k)} \quad (19c)$$

The air-gap flux density and the components of the disc rotor current density have the forms:

$$B_z(r) = j\frac{\mu_o R_s A_s}{p g_s} + j\frac{\mu_o t_c r}{p g_s} J_r \quad (20)$$

$$J_r(r) = D_1 e^{kr} + D_2 e^{-kr} + \frac{c}{K^2} A_s \quad (21)$$

$$J_\varphi(r) = j\frac{Kr}{p}(D_1 e^{kr} - D_2 e^{-kr}) \quad (22)$$

3.4. Radial Distributions

The radial distribution of the gap flux density and disk rotor current density components are shown in *figure. 5, 6 and 7* for different asymmetry of disc rotor by using the *equations 20,21 and 22.* The current density is there normalized by the theoretical base quantity

$$J_o = \frac{\hat{A}_{sm}}{t_c} \quad (23a)$$

and the flux density is normalized by its no load value at the mean stator radius

$$B_o = \mu_o \frac{r_m}{g_s} \hat{A}_{sm} \quad (23b)$$

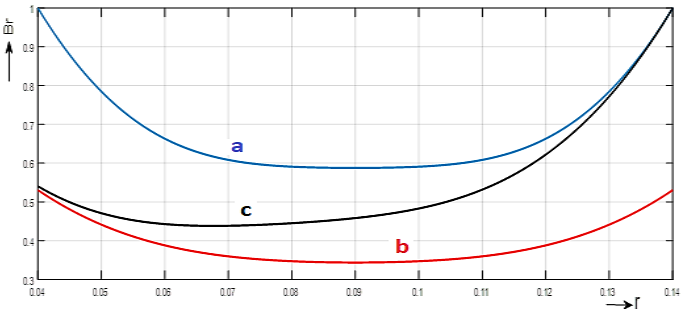

Figure 5. The normalized radial distribution of axial flux density a.Without rotor ends, b. With rotor ends, c. With only inner rotor end

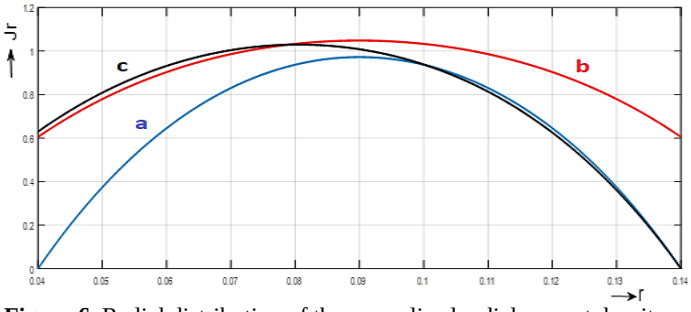

Figure 6. Radial distribution of the normalized radial current density A/Without rotor ends, b. With rotor ends, c. With only inner rotor end

FOREX Publication
Open Access | Rapid and quality publishing
International Journal of Electrical and Electronics Research (IJEER)
Research Article | Volume 12, Issue 2 | Pages 487-492 | e-ISSN: 2347-470X

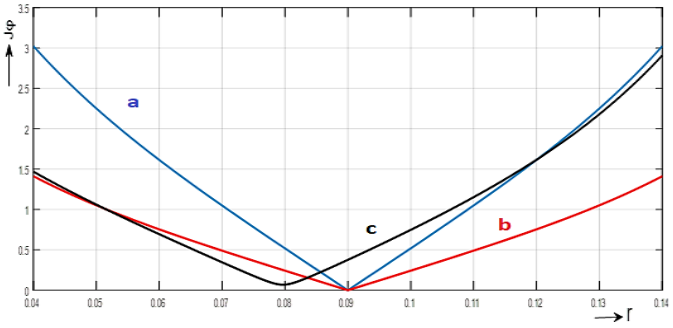

Figure 7. Radial distribution of the normalized tangential current density a. Without rotor ends, b. With rotor ends, c. With only inner rotor end

The flux density and the tangential current density exhibits their minimum values near the middle of the stator, at the same time the radial current density attains a maximum value toward the inner disc end. With unequal out hang lengths or only inner end region, the asymmetry of the distributions becomes more or less strong depending on the length of the end region.

The point of maximum radial current density and those of minimum tangential current density and minimum flux density move towards to longer out hang. These will affect the main performance characteristics of the induction motor with asymmetrical conducting disc rotor.

The computational treatment is based on the solution of field equations written in cylindrical coordinates. The analytical approach described herein leads to a mathematical model, which is also a practical design tool. For accuracy evaluation of the proposed method, the computed results are compared to other results from different papers [1,12,14,15].

4. FORCE AND MOTOR DEVELOPED TORQUE

The force density acting on a unit volume of the rotor disc is given by

$$\vec{F}_v = \vec{J} \times \vec{B} \tag{24a}$$

The tangential force density component is obtained by

$$\vec{f}_{v\varphi} = \frac{1}{2}[J_r . B_z] \tag{24b}$$

with a suitable base f_o for the force density normalization,

$$f_o = \frac{1}{4} B_o J_o \tag{24c}$$

we expected that the maximum torque density value occurs at the inner stator edge. Thus, it is obvious that the asymmetry of the conducting disc rotor will affect the force distribution and hence the resulting motor torque.

A region of higher torque density at r_{si} gives low effect on the developed torque compared to the outer region at r_{so}.
Then, the computed results can be given.

from the previous results, the asymmetry of the conducting disc rotor will affect the force distribution and hence the resulting motor torque. A region of higher torque density at r_{si} gives low effect on the developed torque compared to the outer region at r_{so}.

The integration of the torque density over the disc rotor volume obtains the total torque exerted on the rotor. The motor developed torque can then be obtained by the integration.

$$T = 2\pi t_c \int_{r_{si}}^{r_{so}} f_{v\varphi} . r^2 dr \tag{26a}$$

The normalized torque as function of the motor slip is plotted in *figure 8*. This figure investigates the main characteristics for different dimensions of the disc overhangs with a torque base T_o where,

$$T_o = \pi(r_{so}^2 - r_{si}^2) . t_c . f_o . r_m \tag{26b}$$

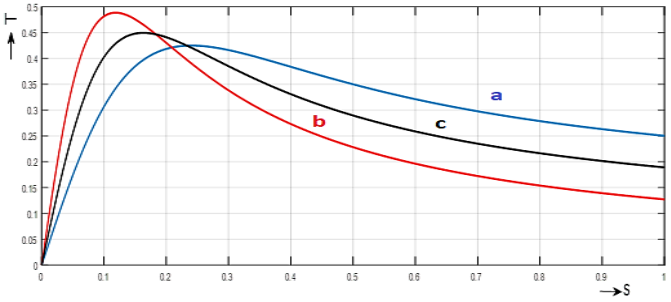

Figure 8. The normalized torque-slip characteristics
a. Without rotor ends, b. With rotor ends, c. With only inner rotor end

Increasing the rotor ends width improves the characteristics of the motor, since more loops of current close their paths through the rotor ends. A better effect is obtained by using asymmetrical overhangs if it is occurred. The longer outer overhang moves the point of maximum force density towards the middle of the stator and results also in obtaining high developed torque in the region of normal operation.

5. CONCLUSION

The disk-rotor induction motor promises a large power density and a small mechanical time constant and make it a suitable choice for servo, Electric Vehicles, Robotics, and high-speed applications.

Using cylindrical coordinates, the analysis of the disc rotor induction motor may need more calculation effort, but it restores the machine geometry as well as the distribution of the field quantities.

This paper introduces a new method avoiding the restrictions, using the boundary conditions that based on well-known methods used for linear induction machines.

The radial distribution of the field quantities and the force density are not uniform and the tangential force density has a maximum value near the inner stator edge. Correspondingly, longer outer overhang leads to improving the characteristics of

FOREX Publication
Open Access | Rapid and quality publishing
International Journal of Electrical and Electronics Research (IJEER)
Research Article | Volume 12, Issue 2 | Pages 487-492 | e-ISSN: 2347-470X

the machine, as the point of maximum force density moves outwards and increases the developed torque. Increasing the width of rotor ends leads to improved machine characteristics. A region of higher torque density at r_si gives low effect on the developed torque compared to the outer region at r_so.

The longer outer overhang moves the point of maximum force density towards the stator middle and results also in obtaining high developed torque in the region of normal operation.

Leakage mechanism of the disc rotor is express decoupling between both stator and rotor windings. the decoupling increases as the ends of the disc rotor decrease since more and more current elements close their paths along the rotor active length.

REFERENCES

[1] WEH, H., MOSEBACH, H. and MAY, H.: "Analysis and characteristics of the Disk - Rotor Induction Motor", electric machines and electro mechanics. 1, 1976, p. 87-98.

[2] HÜBNER, K.D., MOSEBACH, H. and WEH, H.: "A contribution to the calculation of the air gap field of asynchronous linear motors," Etz Archiv 93, 1972, pp. 644-646.

[3] Ahmad Shahid Khan, and Yatendra Pal Singh, Electromagnetics for electrical machines, CRC Press, 2018.

[4] HAGUE, B., The principles of electromagnetism applied to electrical machine, Dover Publications, Inc., New York.

[5] Omar S. Daif, M. Helmy, "Field Analysis, Distribution and Performance of Sleeve Rotor Induction Motor Taking the Sleeve Rings into Consideration ", International Journal of Recent Technology and Engineering (IJRTE), ISSN: 2277-3878, Volume-9, Issue-1, March 2020.

[6] A. B. Kotb "Field Analysis, Distribution and Performance of Sleeve Rotor Induction Motor Taking the Sleeve Rings into consideration", IJRTE, Vol.-9, Issue-1, May 2020, PP. 838 – 842.

[7] Omar S. Daif, A. B. Kotb "Economic design of sleeve rotor induction motor with rotor ends", IJRTE, Vol.-9, Issue-1, Feb. 2021, PP. 838 – 842.

[8] NASAR, S.A.: "An axial - airgap, variable - speed, eddy - current motor", IEEE Transaction. 87, 1968, p. 1599-1603.

[9] J. Law, Jr and D. W. Novotny: "The Two-phase accelerometer", IEEE Trans. -Pas,vol. 83, (1964) 614-619.

[10] A. B. Kotb, "Disc-Rotor Induction Motor with Mechanical Speed Control", Fac. Eng., Ain Shams Univ., No. 4, Vol. 31, Part II, p. 420, 1996.

[11] M. A. Elwany "Two – phase Sleeve Rotor Induction Motor Fed from Single-phase Supply", Journal of Al Azhar University Engineering sector, Vol.6, No.21, October, 2011, 1414-1426.

[12] Salama Abo-Zaid; "Field Analysis and Equivalent Circuit Parameter of Eddy Current Rotor Induction Motor With, Without and Closed Iron Backing", IJAST, Vol. 29, No. 3, 2020, pp. 14109 – 14122.

[13] M. Elwany; "Derivation of the Circuit Parameters for a Sleeve Rotor Induction Machine", JAUES, Vol. 14, Issue 52, 2019: 553-558.

[14] H. May, H. Mosebach, and H. Weh, "Rechnerische Behandlung, Betriebsverhalten und Ersatzschaltbild des asynchronen Scheibenmotors", ETZ-A Bd. 94 (1973) H. 10 pp. 574-577.

[15] A.B. Kotb, M.Shalaby, "Analysis of the Disk Rotor Induction Motor", AMSE Confer. Vol. 2C, PP. 73-86, 1987.